

An aerial photograph showing a large, dark, irregularly shaped area in a light-colored, sandy or silty landscape. The dark area appears to be a mudflow or debris field, possibly the result of a rupture or landslide. The surrounding terrain is light-colored and textured, suggesting a sandy or silty surface. The dark area is roughly rectangular but has jagged, irregular edges. There are some smaller, lighter-colored patches within the dark area, and some small, dark spots scattered throughout the light-colored terrain.

**Rupture propagation in
2 – D fault models**



Numerical Method: BIE 2 - D

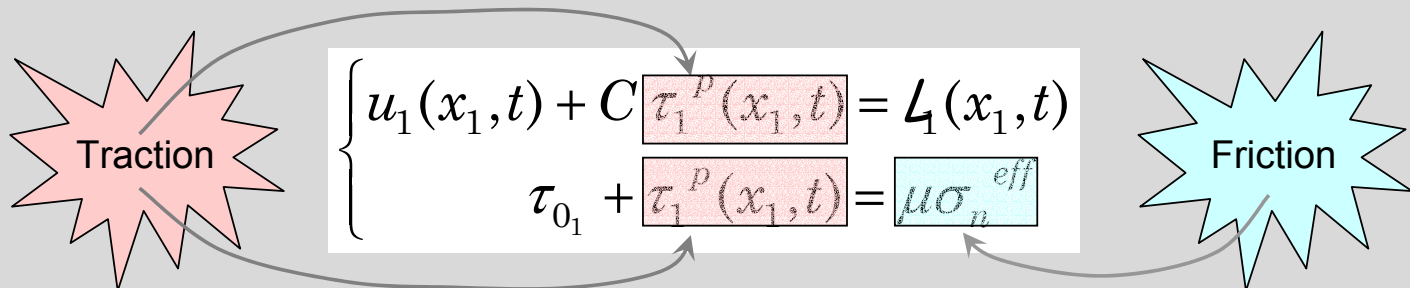
We solve the fundamental elastodynamic equation, neglecting body forces \mathbf{f}

$$\rho \ddot{U}_i = \sigma_{ij,j} + f_i$$

Source integral representation (*Betti*' s theorem, Integration in time limit in fault surface, Lamb' s problem):

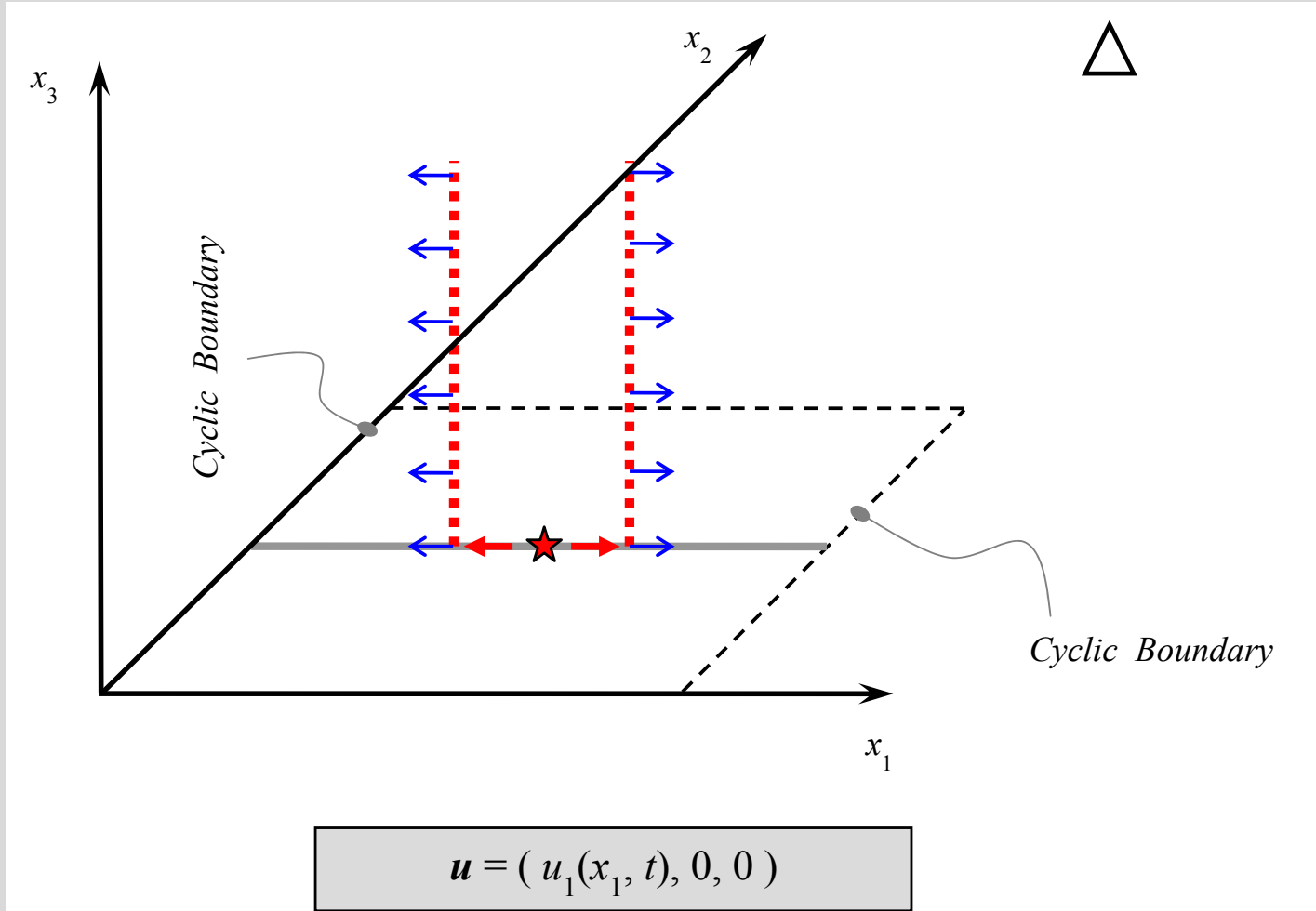
$$u_n(\mathbf{x}, t) = \int_{-\infty}^{+\infty} dt' \int_{S(t')} d\xi G_{n\alpha}(\mathbf{x} - \xi, t - t') \sigma_{\alpha\beta}^p(\xi, t'); n=1,2,3; \alpha=1,2; \mathbf{x}, \xi \in \mathbb{R}^3$$

First neighbours decoupling (in the case of a 2 - D, pure in - plane rupture):





Numerical Method: FD 2 - D



We solve the fundamental elastodynamic equation, neglecting body forces \mathbf{f}

$$\rho \ddot{u}_i = \sigma_{ij,j} + f_i$$

We discretize the $x_1 x_2$ plane by using triangular cells (better performances)

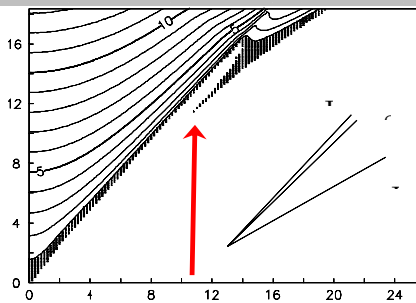
$$\rho \frac{\partial}{\partial t} \dot{u}_1 = \frac{\partial}{\partial x_1} \Sigma_{11} + \frac{\partial}{\partial x_2} \Sigma_{12}$$

$$\rho \frac{\partial}{\partial t} \dot{u}_2 = \frac{\partial}{\partial x_1} \Sigma_{12} + \frac{\partial}{\partial x_2} \Sigma_{22}$$

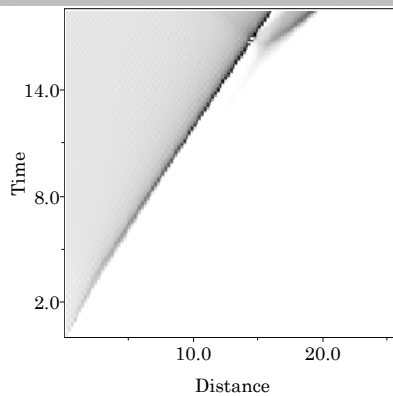
The plane is linear and elastic except in the fault intersection line, where a Fault Boundary Condition (TSN scheme) is adopted. In this line a constitutive law is assumed to relate staggered stress with observables (slip, slip velocity, ...)

BIE vs. FD with SW #1

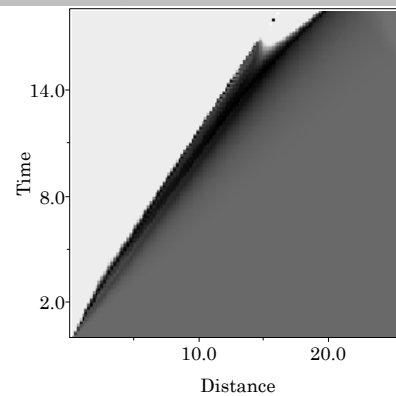
BIE



(a)

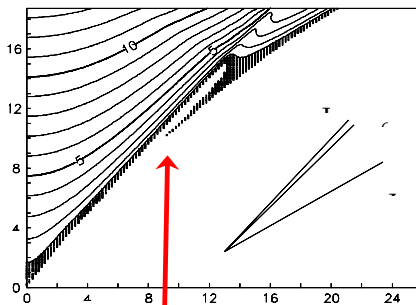


(b)

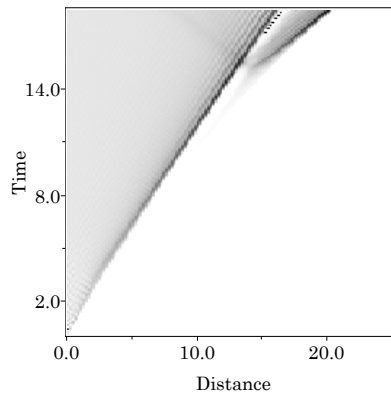


(c)

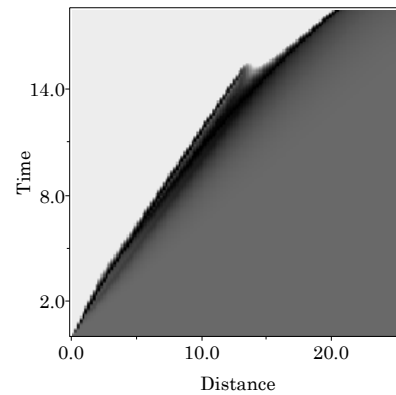
FD



(d)



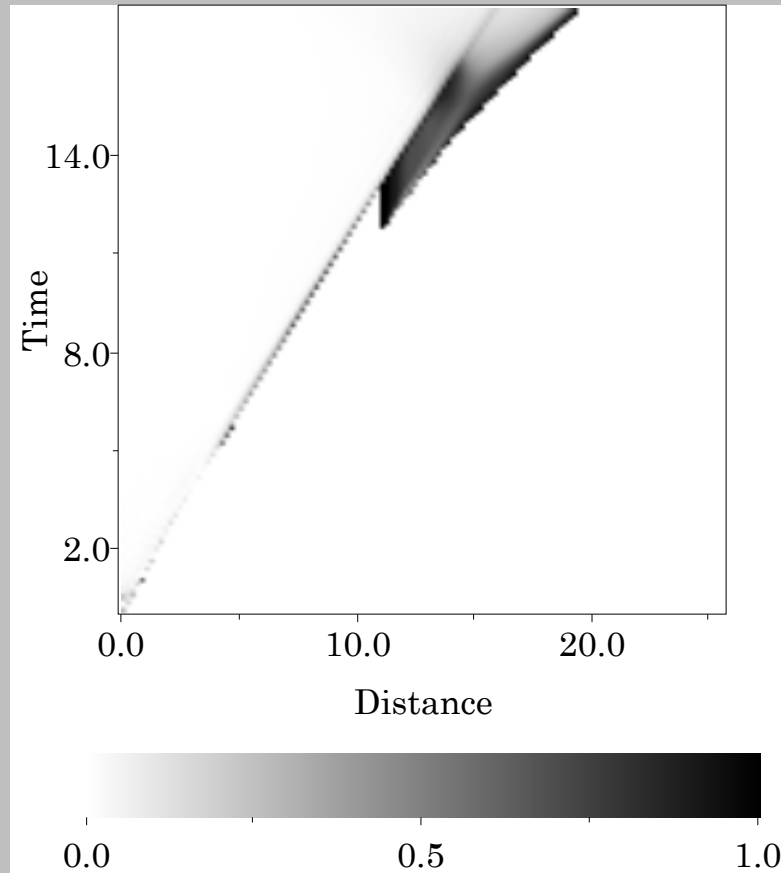
(e)



(f)

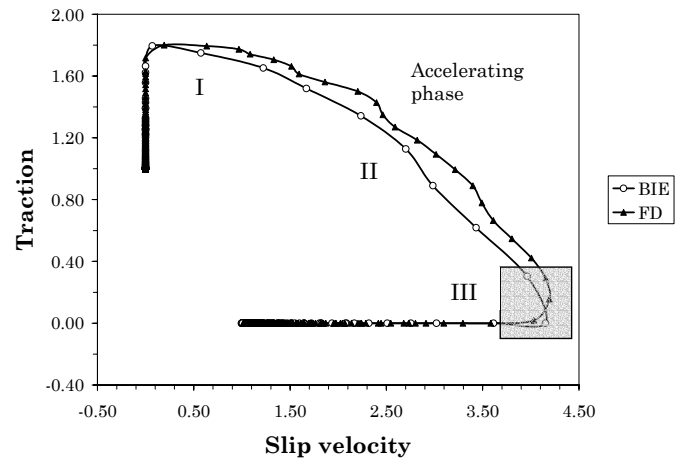
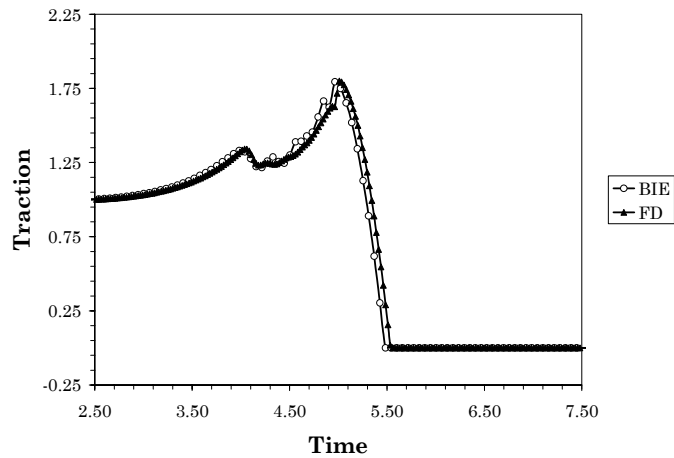
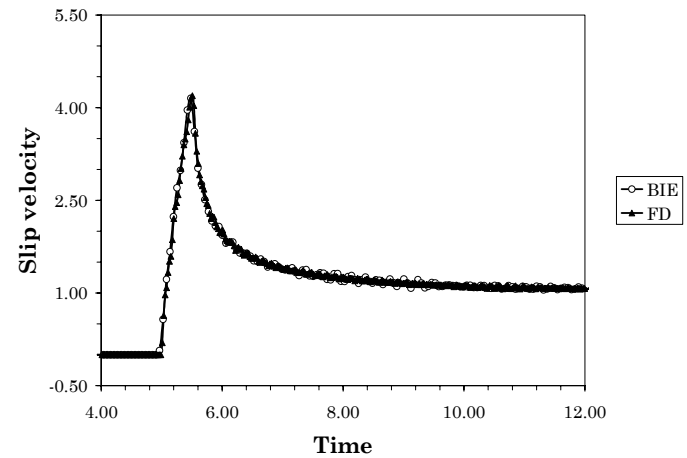
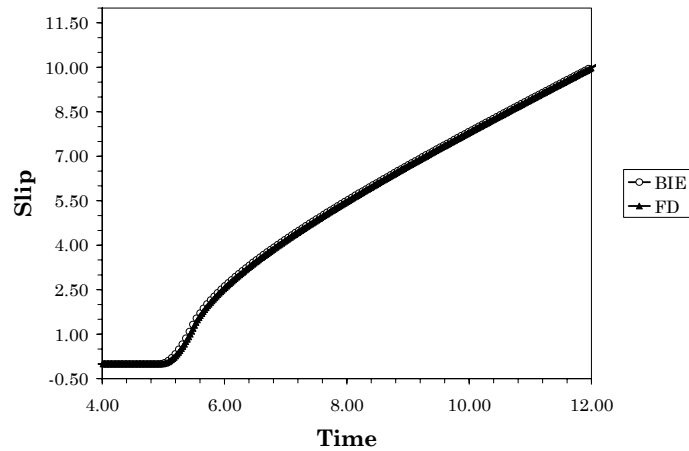
Misfit between slip modeled with BIE and FD

$$m(x_i, t_n) = \frac{\left| u^{(\text{BIE})}(x_i, t_n) - \tilde{u}^{(\text{FD})}(x_i, t_n) \right|}{\left| u^{(\text{BIE})}(x_i, t_n) + \tilde{u}^{(\text{FD})}(x_i, t_n) \right|}$$

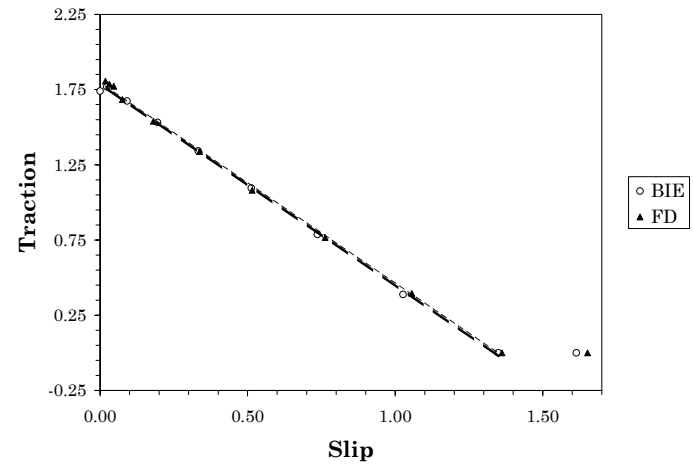
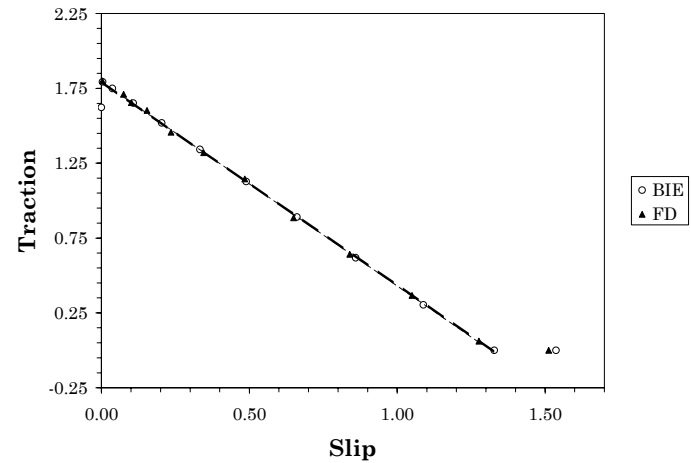




BIE vs. FD with SW #2

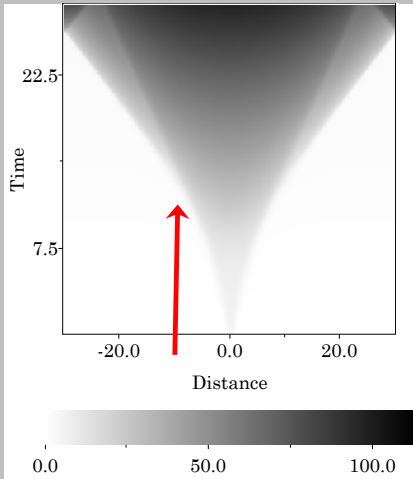


BIE vs. FD with SW #3

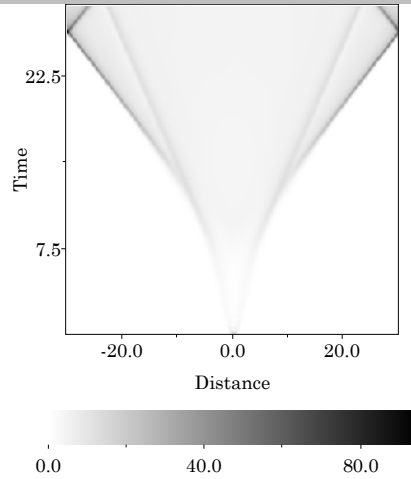




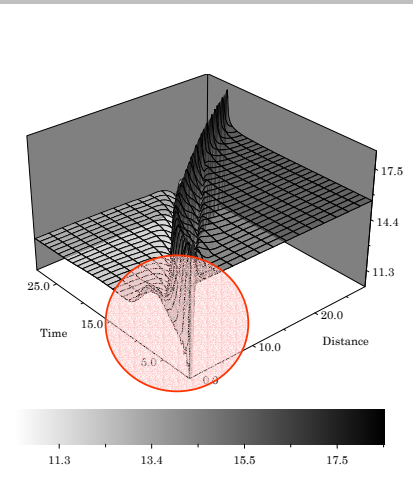
SW vs. DR law #1



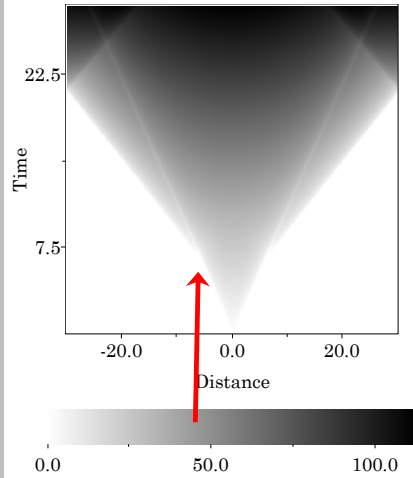
(a)



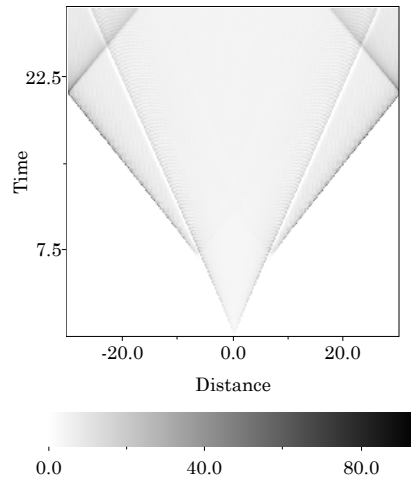
(b)



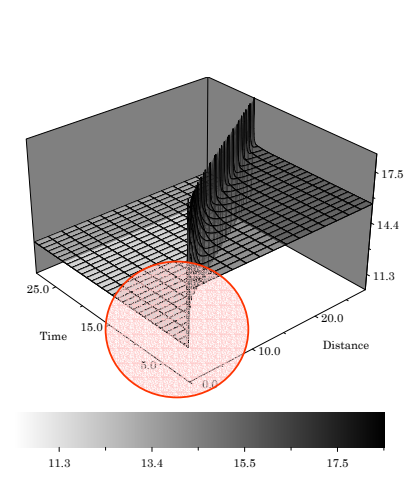
(c)



(d)

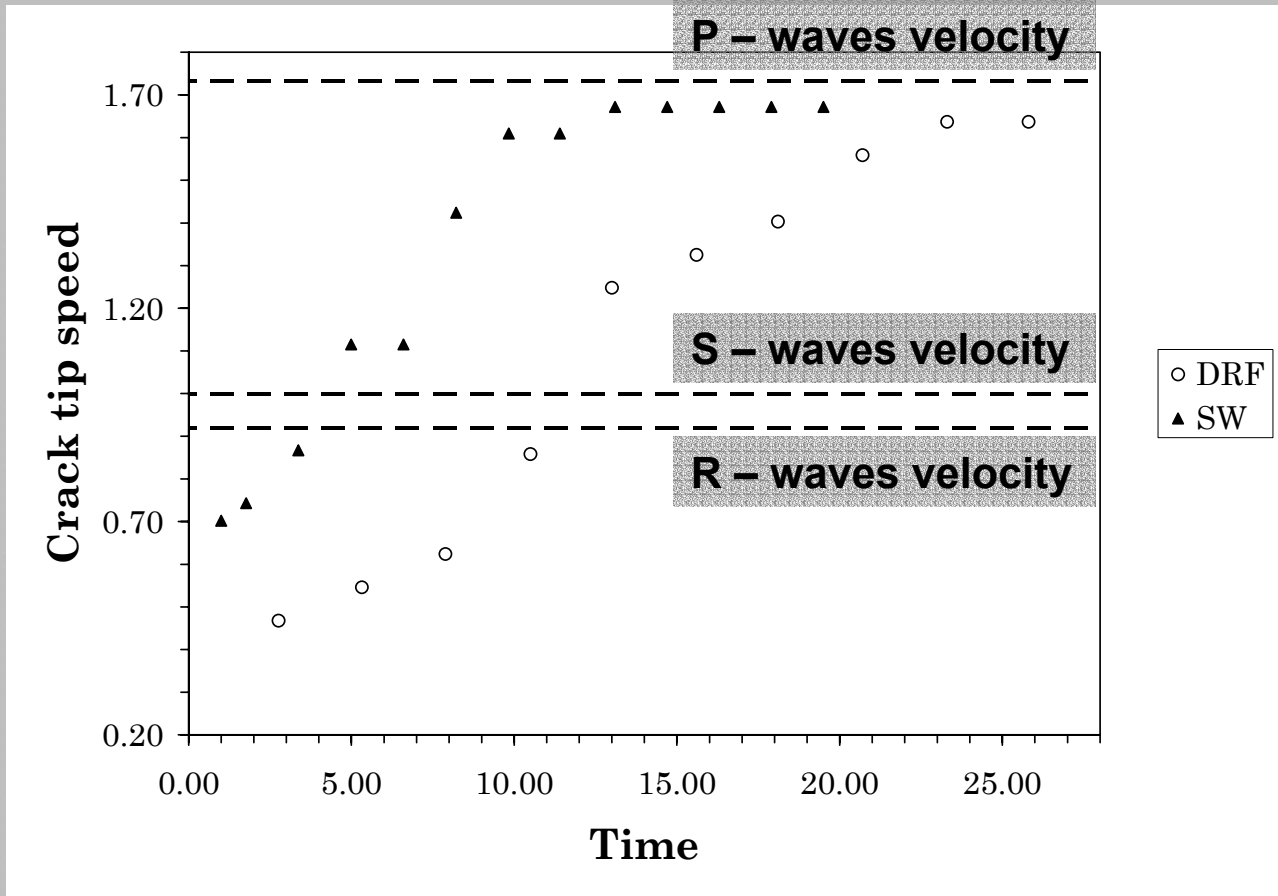


(e)

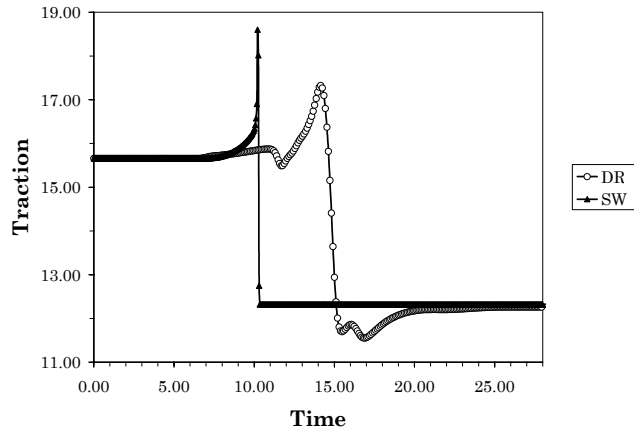


(f)

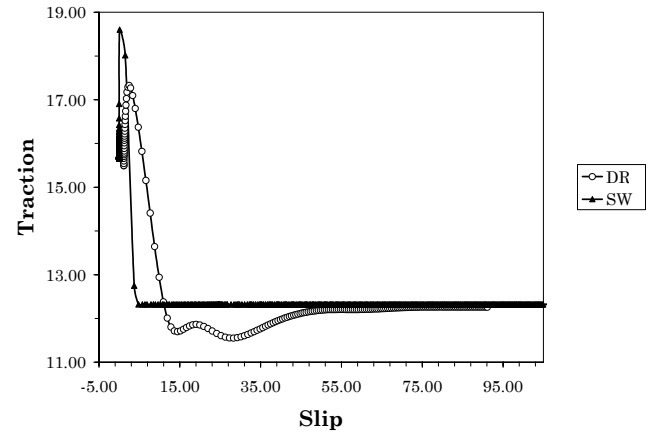
SW vs. DR law #2



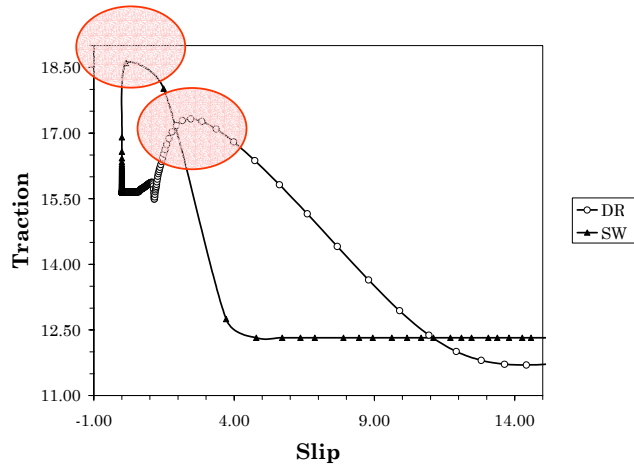
SW vs. DR law #3



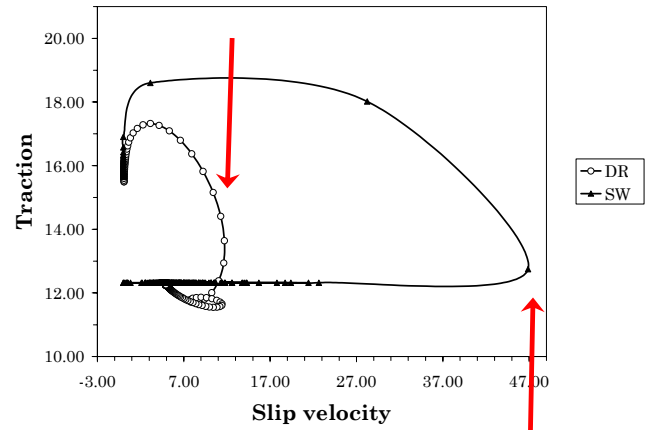
(a)



(b)

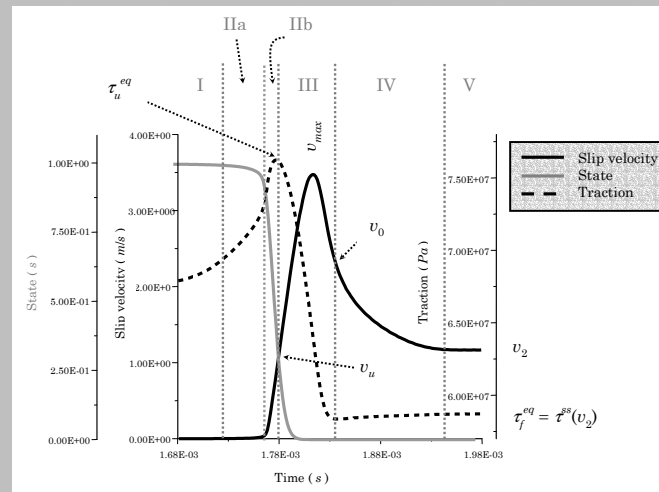
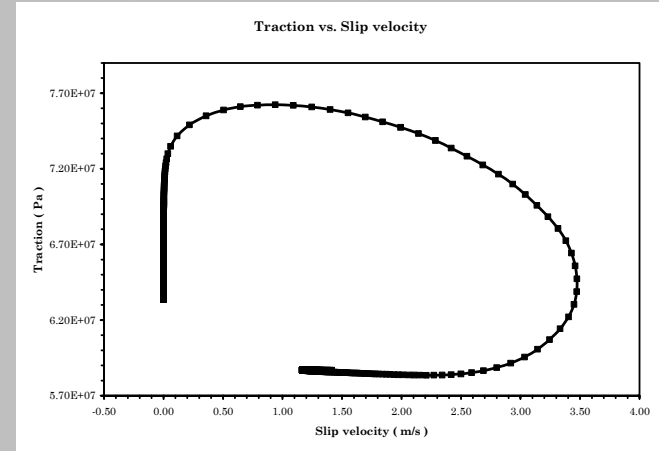
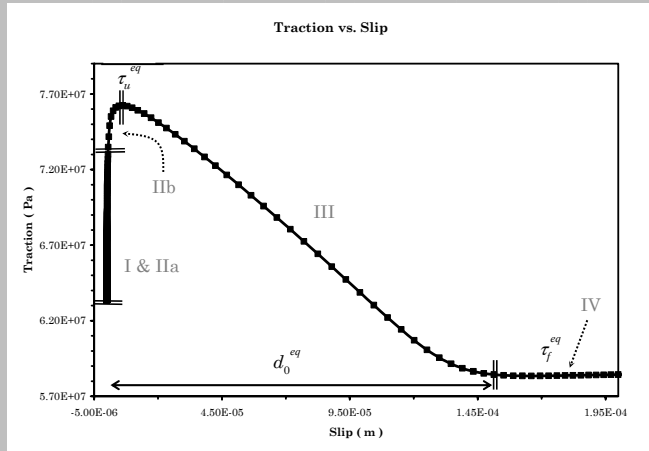


(c)

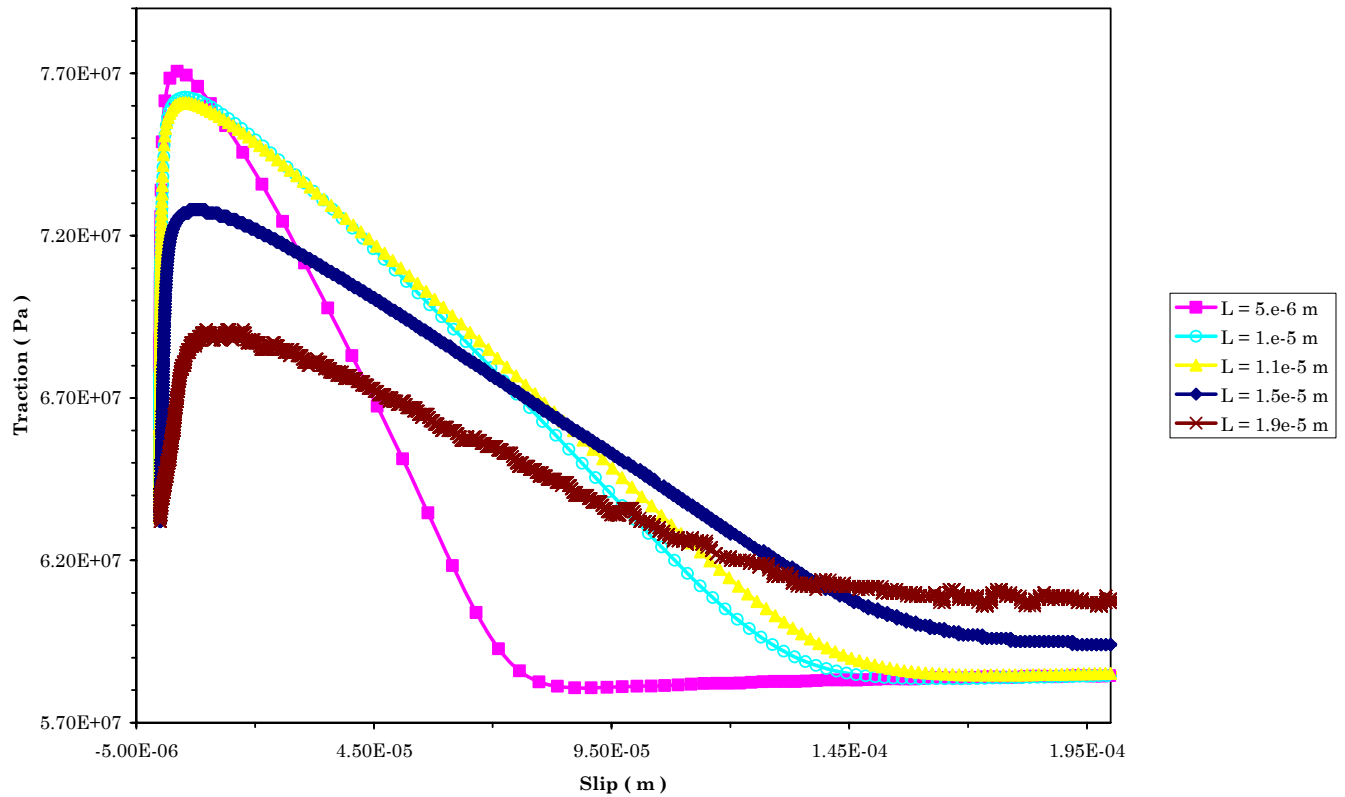


(d)

The dynamic propagation. The cohesive zone and the breakdown



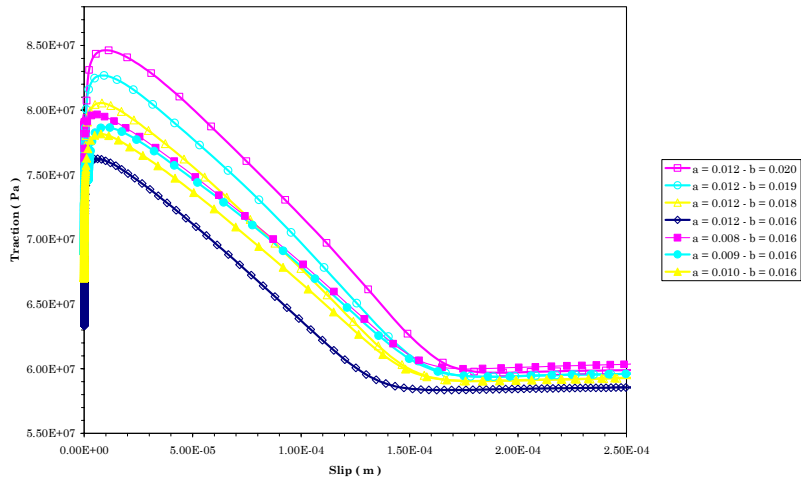
Dependence on L parameter



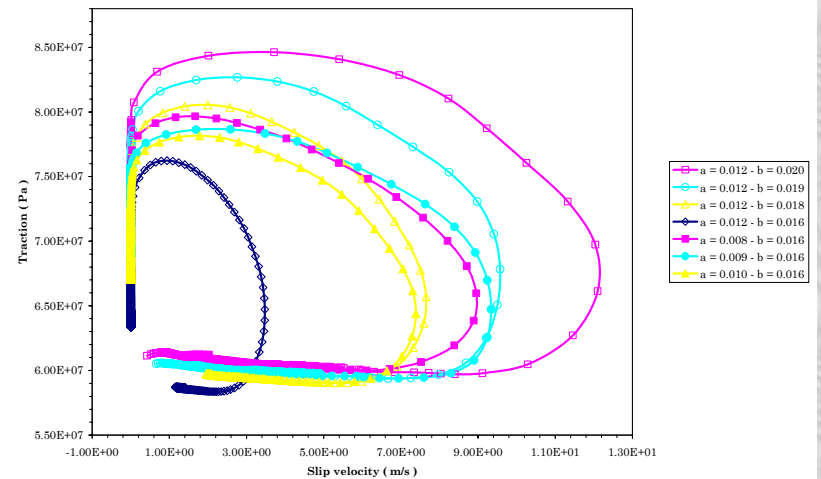


Dependence on a and b

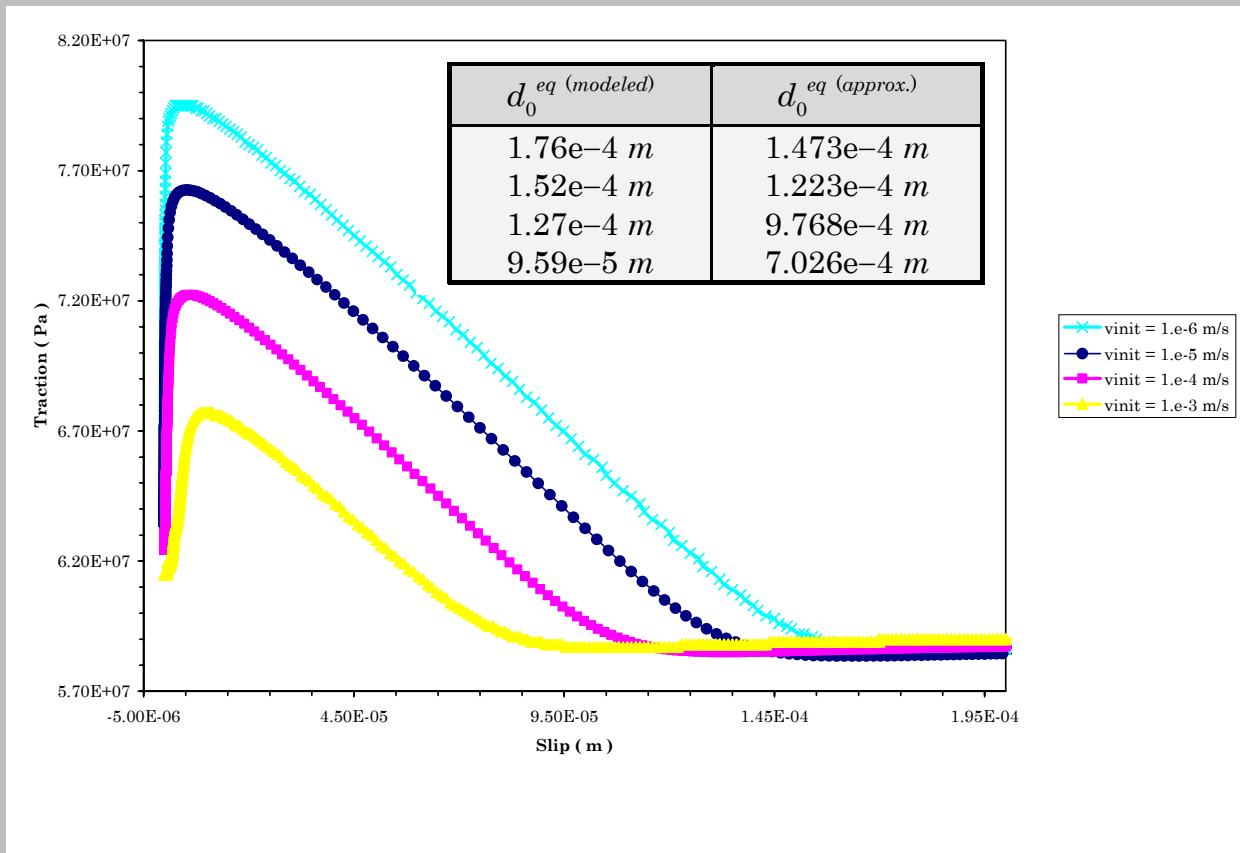
Slip – weakening curves



Phase portraits



Dependence on the initial velocity



Limitation for modeling dynamic Rupture and seismic wave generation

- Because the initial slip velocity is totally arbitrary, it is difficult in the framework of R&S formulation to prescribe the traction evolution and the **SW** behavior within the cohesive zone.
- We can only infer an approximated value of the equivalent slip – weakening distance from the proposed scaling law. Moreover, the difference between d_0^{eq} and L depends on the adoption of a slowness (ageing) evolution equation.

Theoretical interpretations

➤ We derived analytical expressions that relate the yield and the kinetic frictional stresses to the constitutive parameters and to slip:

$$\tau = \left[\mu_* + a \ln\left(\frac{v}{v_*}\right) + b \ln\left(\frac{v_*}{v_{init}}\right) - b \frac{u}{L} \right] \sigma_n^{eff}$$

$$\tau_f^{eq} = \left[\mu_* + (b - a) \ln\left(\frac{v_*}{v_2}\right) \right] \sigma_n^{eff}$$


$$D_0^{eq} = L \ln\left(\frac{V_0}{V_i}\right) \approx \frac{\tau_u^{eq} - \tau_f^{eq}}{b \sigma_n} L$$

➤ These relations hold under the assumptions that and that slip velocity is large enough to neglect the term $1/v$. This yields

$$\phi(u) = \frac{L}{v_{init}} e^{-\frac{u}{L}}$$

Numerical estimates of characteristic length

- Laboratory experiments:

Laboratory scale  fault dimension $\sim 20 \text{ m}$ $\Delta x \sim 0.01 \text{ m}$ $L \sim 10^{-5} \text{ m}$
 $L \sim 10^{-5} \text{ m}$ $d_0^{eq} \sim 10^{-4} - 10^{-3} \text{ m}$

- Extending our calculations to real faults

✓ Estimates of D_0 from ground motions or kinematic source models range within $0.5 \leq d_0 \leq 1 \text{ m}$.

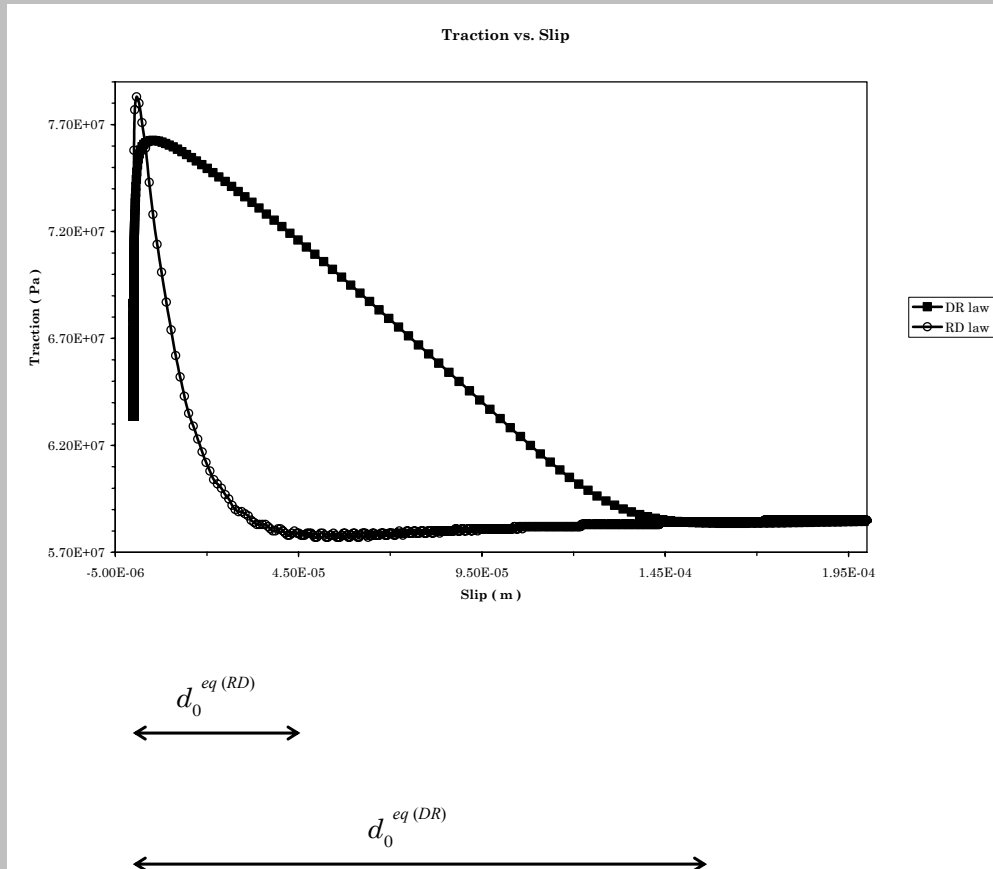
[*Ide and Takeo, 1997; Olsen et al., 1997; Guatteri and Spudich, 2000*]

✓ There is a trade - off between strength - excess and the slip weakening distance d_0 [$d_0 < 0.3 \text{ m}$ are not resolved]

✓ Estimate of d_0 inferred from kinematic inversion models are biased due to smoothing constraints used in the inverse - problems formulation [*Guatteri and Spudich, 2000*]

Fault scale  fault dimension $\sim 20 \text{ km}$ $\Delta x \sim 10 \text{ m}$ $L \sim 10^{-2} \text{ m}$
 $L \sim 10^{-2} \text{ m} = 1 \text{ cm}$ $d_0^{eq} \sim 10^{-1} \text{ m}$

Differences between DR and RD



This slide is empty intentionally.

